Magnetic contrast agents for optical coherence tomography

Amy L. Oldenburg[a,c], Jillian R. Gunther[a,c], Farah Jean-Jacques Toublan[b,c], Daniel L. Marks[a,c], Kenneth S. Suslick[b,c] and Stephen A. Boppart[a,c*]

[a] Department of Electrical and Computer Engineering, University of Illinois at Urbana-Champaign, 1406 W. Green St., Urbana, IL 61801

[b] Department of Chemistry, University of Illinois at Urbana-Champaign, 600 N. Mathews Ave., Urbana, IL 61801

[c] Beckman Institute for Advanced Science and Technology, University of Illinois at Urbana-Champaign, 405 N. Mathews Ave., Urbana, IL 61801

ABSTRACT

The magneto-mechanical effect is exploited as a means of producing background-free contrast in optical coherence tomography (OCT). Contrast agents consisting of iron-oxide particles and protein microspheres encapsulating colloidal iron-oxide have a sufficiently high magnetic susceptibility to be detected by modulation of a magnetic field gradient using a small solenoid coil. The externally-applied magnetic field mechanically rotates or translates these highly scattering contrast agents within the sample at the modulation frequency, which is subsequently detected as amplitude modulation of the OCT signal. Pairs of sequential axial scans (A-lines) are acquired with the magnetic field on and off, allowing one to build up a pair of images corresponding to the "on" and "off" states of the magnetic field. These image pairs are differenced to look for magnetic-specific effects, allowing one to distinguish the magnetic contrast agents from non-magnetic structures within the sample with a signal-to-background ratio of ~23dB. This technique has the potential to be very powerful when coupled with targeting for *in vivo* molecular imaging. To evaluate this potential we demonstrate *in vitro* imaging of magnetically-labeled macrophage cells embedded in a 3D tissue phantom, *in vitro* tissue doped with contrast agents, and *in vivo* imaging of *Xenopus laevis* (African frog) tadpoles.

Keywords: contrast agents, optical coherence tomography, magnetomechanics.

1. INTRODUCTION

Contrast agents have been developed for every biomedical imaging modality to enhance the diagnostic capabilities, whether it be through overall image enhancement or by providing functional information through selectivity. The use of topical hyperosmotic agents such as glycol[1] have proven effective for increased depth penetration and contrast in OCT imaging of skin and highly-scattering gastrointestinal tissue. The development of injectible, functionalizable contrast agents for molecular imaging is a major goal in biomedicine today[2]. One means of achieving this in OCT is the use of highly scattering contrast agents which, when targeted to the molecule of interest, produce an enhanced signal at tissue sites expressing the molecule. Some promising agents which have been tailored to exhibit large scattering amplitudes at the near-infrared wavelengths typically used for OCT include phospholipid micro air bubbles[3] and engineered protein microspheres incorporating nanoparticles in their shell[4]. However, the premise of this means of contrast enhancement is that the backscattered signal from the agents must be sufficiently large with respect to the background from the tissue itself. Although these agents can be used to increase contrast, in order for these to be useful for molecular imaging, it would be necessary to know what the state of the tissue is before application of the contrast agents; in other words, in order to distinguish the agents from background tissue one must either build up a knowledge database of normal tissues, or acquire pre-injection control images for every sample to be studied. This could potentially be time-consuming if one does not know which tissue of interest may eventually be targeted by the agents.

One way to address this problem is to use agents that are dynamically controllable such that they can be easily distinguished from the tissue itself. We present here a means of contrast agent detection through the magneto-mechanical effect, that is, the induced movement of the agents through an externally-applied magnetic field. In such a scheme it is not necessary that the agents scatter with an appreciable signal but only that they modulate their own

* Send correspondence to S. A. Boppart, E-mail: boppart@uiuc.edu, Telephone: 1 (217) 244-7479

Coherence Domain Optical Methods and Optical Coherence Tomography in Biomedicine VIII, edited by Valery V. Tuchin, Joseph A. Izatt, James G. Fujimoto, Proc. of SPIE Vol. 5316 (SPIE, Bellingham, WA, 2004) · 1605-7422/04/$15 · doi: 10.1117/12.529119

scattering properties or the scattering in their local environment (by, *e.g.*, moving neighboring cell membranes and nuclei). There is a large wealth of knowledge on synthesizing biocompatible magnetic agents used extensively in MRI[5] and recently as probes in fluorescence microscopy[6]. Therapeutically, magnetic agents show promise for inducing hyperthermia at tumor sites under magnetic fields modulated at frequencies >100kHz[7], and have been used to selectively lyse targeted cells *in vitro* under intense (>5T) static magnetic fields[8]. The quality factor in magnetomechanical contrast agents is primarily the magnetic susceptibility, which dictates the force with which a material responds to a magnetic field gradient. This is, in fact, the same quality desired in therapeutic agents for hyperthermia, and is also compatible with the requirements for other imaging modalities allowing for multi-modal contrast agent development[9]. In this work, two types of contrast agents were investigated. The first are randomly-shaped micron-sized magnetite (Fe_3O_4) particles (Sigma #3110069). The second are sonochemically-generated albumin microspheres which encapsulate a vegetable oil-based 10% w/v hematite (Fe_2O_3) colloid. The latter agents have also proven successful as MRI contrast agents (by ferromagnetically-induced signal loss) within the mononuclear phagocytic system in the liver and spleen. Similar sonochemical protein microspheres have been shown to be highly biocompatible with a long circulation time[10]. Below we outline the mechanism of contrast enhancement for OCT and present realizations of this technique *in vitro* in cells and tissues, and *in vivo* in a *Xenopus laevis* (African frog) tadpole.

2. BACKGROUND

2.1 Magneto-mechanics

Magnetite ($Fe^{(II,III)}{}_3O_4$) in bulk form is known to be ferrimagnetic, which is characterized by a remanent magnetic field arising from unopposed spin from Fe(II) atoms. Hematite (α-$Fe^{(III)}{}_2O_3$) exhibits antiferromagnetism at room temperature, which is characterized by antiparallel spins resulting in behavior at fixed temperature similar to paramagnetism. Ferro- and ferrimagnetic particles experience torque upon exposure to a magnetic field, which can be expressed as:

$$\vec{\tau} = V\vec{M} \times \vec{B} \tag{1}$$

where V is the particle volume, M the internal magnetization, and B the applied field. If the particle is free to move, it will physically rotate until its internal field is aligned with the applied field.

As the magnetic particle size is decreased to the order of a magnetic domain[5], the particles typically lose their remanent field and are more accurately described as superparamagnetic. One consequence is that the internal magnetization, M, will align freely with an applied field without the need for physical rotation, and hence no torque is experienced. Although superparamagnetic agents will not experience torque, they do experience translational forces when exposed to a magnetic field gradient, which can be expressed as:

$$\vec{F} = \frac{V(\chi_m - \chi_0)\nabla B^2}{2\mu_0} \tag{2}$$

where χ_m and χ_0 are the magnetic susceptibilities of the contrast agent and the background, respectively. This force is experienced by both ferromagnetic and superparamagnetic agents, and always points in a direction toward increasing magnetic flux, independent of the polarity of the field. For a 1-micron diameter magnetite particle (χ_m=0.2) under a field magnitude and gradient of 1 T and 10 T/m, respectively, this force can be estimated as 0.8 pN. This is on the same scale as the forces necessary for optical trapping and optical tweezer experiments[11].

We expect that the micron-sized magnetite particles used as contrast agents in this study will experience both torsional and translational forces as outlined above, with a susceptibility comparable to that of the bulk material (χ_m=0.2). The second type of contrast agents studied here are albumin microspheres encapsulating colloidal hematite in vegetable oil. Although the overall sphere sizes are large (1-5μm), these encapsulated hematite particles are nominally 10nm (as characterized by SEM), sufficiently small to be within the superparamagnetic regime. Figure 1 illustrates magnetometry performed using a SQUID (superconducting quantum interference device) of the colloidal hematite which suggests a susceptibility on the order of $7*10^{-4}$. It also illustrates that this material exhibits negligible remanent field.

In general we expect the background magnetic susceptibility χ_0 to be negligible with respect to these magnetic contrast agents[12]. The torques and translational forces as described above will act to mechanically move the contrast agents. The amount of rotation or translation will depend upon the visco-elastic properties of the tissue or cellular compartments

containing the agents, in addition to the strength of any bonding sites (chemical, electrostatic) between the particle and tissue.

2.2 OCT detection of magnetomechanical motion

There are several primary mechanisms illustrated in Fig. 2. by which a rotating or translating particle can be detected using OCT. OCT is based on a Michelson interferometer, where the sample (in this case, the contrast agent) is placed in one arm of the interferometer, and the optical delay of a retroreflecting second arm (the reference arm) is swept so as to optically range the coherently backscattering particles within the sample. The interferogram generated at the output of the interferometer is characterized by fringes at the Doppler frequency induced by the moving reference arm. The amplitude of the complex analytic signal produced by taking a Hilbert transform of this interferogram (essentially the envelope of the fringe data) gives spatial information about the structure of the sample.

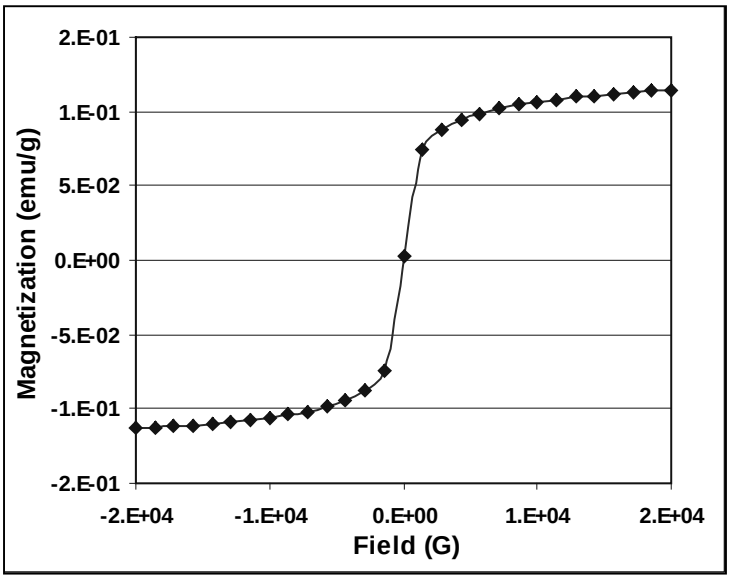

Fig. 1. SQUID magnetometry of hematite colloid 10% *w/v* in vegetable oil prepared by precipitation of ferric and ferrous chloride. This solution is encapsulated in albumin microspheres for use as a magnetic contrast agent for OCT.

As shown in Fig. 2, the OCT interferogram can be changed in amplitude or phase depending on the mechanism for particle movement. In this experiment a solenoid with small inner radius (1cm) was used which is expected to induce significant translational forces (by Eqn. 2) in both the transverse and axial directions. Also, the magnetite particles used as contrast agents were significantly anisotropic so that one might expect rotation to add significantly to the magnetic-dependent contrast.

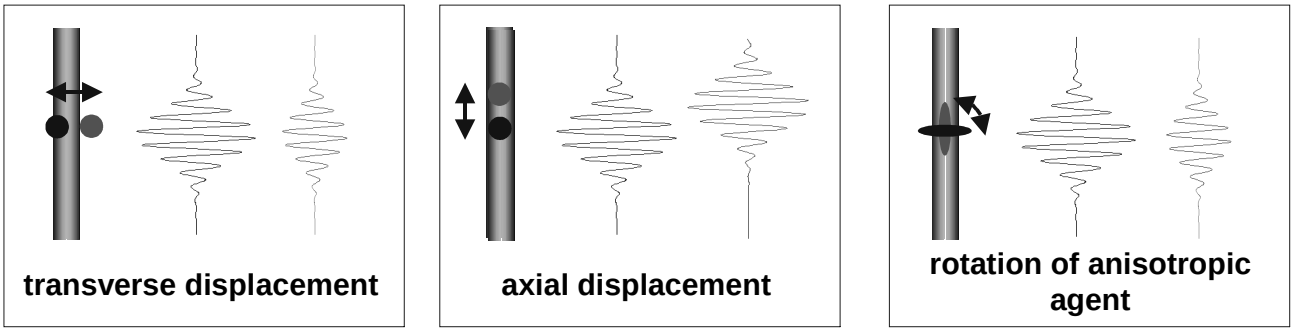

Fig. 2. Simplified diagrams of the movement of a single magnetic contrast agent particle and the resulting OCT fringes. In each diagram, the particle moves in a direction indicated by the arrows. The resulting interferograms for the particle in each of two positions is shown to the right in each diagram. Left: Transverse displacement is characterized by a change in the amplitude of the OCT interferogram. Middle: Purely axial displacement is characterized by a shift of the center of the interferogram (a phase shift), but can also induce an amplitude change due to the finite confocality of the beam. Right: Rotation of a non-spherical particle results in an amplitude change just as it does for transverse displacement.

In OCT, this movement can be detected by acquiring sequential axial scans (A-lines) while a magnetic field gradient is switched on and off. Axial movement can be detected by cross-correlating the amplitudes of these A-lines, and transverse movement can likewise be detected by cross-correlating the resulting two images (collections of A-lines with the field on and off) along the transverse axis. It is interesting to note that "walk-off" can occur as the magnetic field is switched on and off, that is, the particles do not always return to the same state when the field is off. It has been observed that magnetic contrast agents in a low-viscosity liquid environment will drift in the direction of the strongest

magnetic field density. In general this movement can still be detected by the same means as particles that do not walk off. However, the walk-off appears to be negligible in solid tissues and agarose tissue phantoms.

Purely rotational movement will only produce a change in amplitude at the location of the scatterer. Using light microscopy, magnetite contrast agents in aqueous solution were observed to primarily rotate under a switched axial magnetic field, where the particle cross-sections in the transverse plane were minimized when the field was on (the long axes of the particles would align with the field). Using OCT, both possible effects (centroid movement and amplitude modulation) were observed independently on various magnetite particles embedded in a 5% *w/v* agarose gel. An effective displacement (if the mechanism is transverse displacement) of ~1μm could be inferred using knowledge of the beam waist diameter. Further investigation is necessary, however, to determine if the amplitude modulation effect is due to rotation or to movement in the transverse plane.

One simple means of imaging the magnetically-induced movement which accounts for all three mechanisms is to take the difference between corresponding pixels from sequential A-lines (field on/field off) using the following formula:

$$signal = \frac{(a_{on} - a_{off})^2}{a_{on} + a_{off}} \tag{3}$$

where a_{on} and a_{off} are the amplitudes of corresponding pixels in sequential A-lines, and the denominator is normalization to account for shot noise.

From the above discussion it is apparent that a large field magnitude and gradient are desired to produce significant movement for detection by OCT. Considering typical OCT imaging geometries, a solenoidal coil for use as an electromagnet was designed to 1) allow a 1-cm central hole for passage of the laser to the tissue for imaging, and 2) maximize the magnetic field magnitude and gradient at a distance of ~2 mm above the coil surface (specifically, to maximize ∇B^2). Finite-element calculations suggest an optimal coil outer diameter of 18 mm and height of 9 mm (see Fig. 3) which were relatively independent of the wire gauge used. A coil was made to these specifications, operated at 100 W with a 25% duty cycle, and water-cooled to prevent overheating. The water-cooling sheath allows samples to be placed as close as 1mm from the plane defined by the coil surface. The maximum axial field magnitude and gradient measured with a Hall teslameter 5 mm from the imaging region were 0.019 T and 3.5 T/m at a reduced operating power, and are extrapolated to be 0.11 T and 17 T/m (with ~23% nonuniformity in ∇B^2 over a 1mm by 1mm area) within the imaging region when operated at the full 100 W. The measured results are within 10% of the predicted values, suggesting that the non-uniformity in ∇B^2 over the imaging volume can be easily corrected for in post-processing these magnetic images.

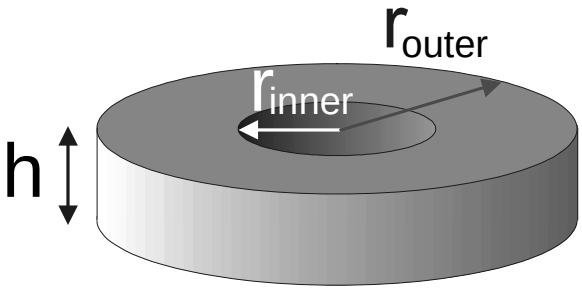

Fig. 3. Diagram of solenoid constructed for magneto-mechanical OCT imaging illustrating the parameters that were optimized to deliver the maximum force to the contrast agents.

3. EXPERIMENT

A fiber-based OCT system with a galvanometer-based delay arm (see Fig. 4) was operated between 10 and 40 Hz for this study. The titanium:sapphire laser source was wavelength-broadened to nominally 100nm FWHM at a center wavelength of 800 nm by using an ultrahigh-numerical aperture fiber[13], corresponding to an axial resolution of typically 3μm. The sample arm lens was an f=20mm achromat resulting in a transverse resolution of about 8μm. Samples to be imaged were placed immediately above or below the solenoid described previously, with the imaging region centered on the axis of the solenoid to maximize the axial field gradient. The solenoid current was switched on during alternate A-lines as indicated, and images were over-sampled in both the transverse and axial directions.

To demonstrate the ability to track labeled cells *in vitro*, macrophages (designation J774A.1) were labeled with magnetic agents and dispersed into a 5% w/v low-gel temperature agarose containing cell media (DMEM). The magnetite sample contained macrophages which had been incubated with micron-sized magnetite particles overnight and rinsed. Counting

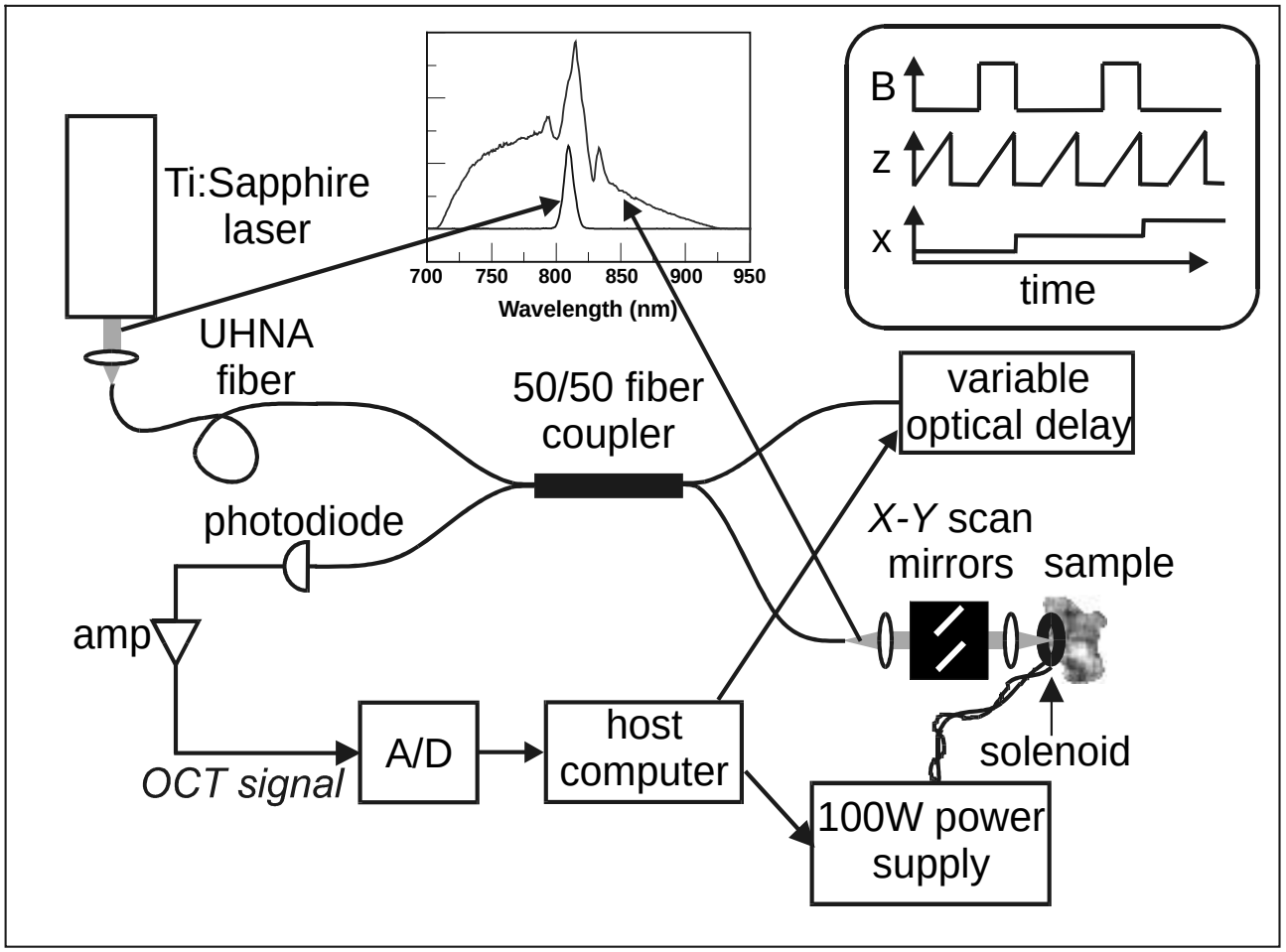

Fig. 4. Diagram of magnetic OCT experimental apparatus. The top central graph illustrates the laser spectrum before and after broadening in the UHNA fiber. Galvanometer mirrors scan the sample transversely while a galvanometer-mounted retroreflector provides optical delay. The computer synchronizes the A-lines to the solenoid coil power supply such that the magnetic field is switched on and off with each successive A-line, as illustrated in the upper right inset.

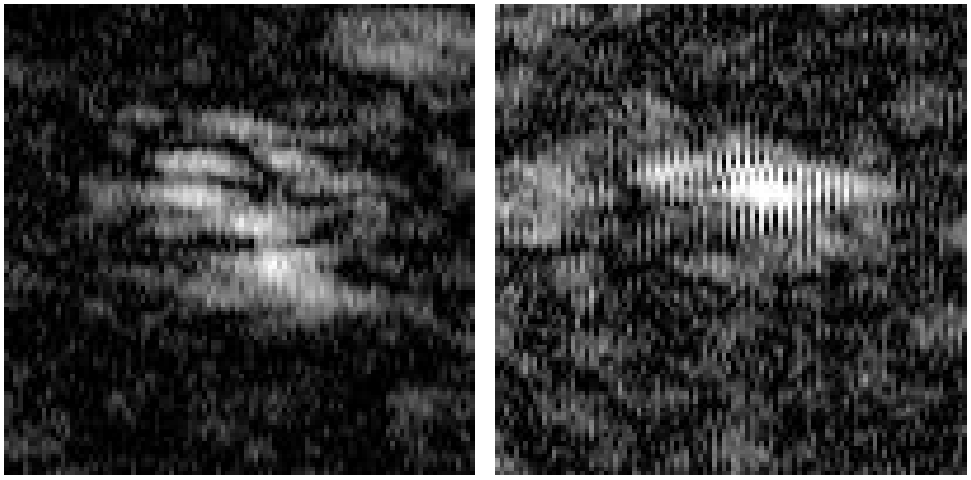

Fig. 5. 65μm x 65μm OCT images of a macrophage cell embedded in agarose-based tissue phantom with a switching magnetic field applied during alternating A-lines. Left: Control cell. Right: Cell that has been exposed to magnetic contrast agents. The influence of the magnetic field can be observed in the modulated structure of the A-lines, which suggests that this cell is in physical contact with magnetic contrast agents (likely via phagocytosis).

revealed ~50% of the cells contained magnetite immediately before detachment and dispersion into gel. A control

sample was prepared similarly without introduction of magnetite. OCT structural and magnetic images of both samples were obtained using Eqn. (3), and show that, as expected, ~50% of the magnetite-labeled cells visible in the structural image appear to have a significant magnetic signal, whereas none of the control cells do. Fig. 5 illustrates an image of one such magnetically-labeled cell at sufficiently high magnification to see the modulation of the amplitude with successive A-lines. It is interesting to note that the shot-noise normalization of Eqn. (3) is necessary to eliminate unwanted background signal from structures such as the agarose surface. By comparing the maximum signal obtained from the magnetic sample to the rms signal from the control image, we estimate the signal-to-noise ratio (SNR) to be ~16dB.

In vitro tissue studies were carried out in three samples of chicken skin: one control was soaked in saline, and the other two samples were topically treated with the contrast agents (magnetite particles or albumin microspheres containing hematite colloid) suspended in saline. Fig. 6 illustrates the magnetic-specific OCT images of the two magnetic samples in comparison to the control. The control sample did exhibit some background, which is attributed to movement of the transverse scanning mirror between consecutive A-lines (as verified by the transverse cross-correlation). This has subsequently been corrected so that the mirror scans as depicted in Fig. 4, with subsequent control images of *in vitro* samples demonstrating a complete absence of background. Although the magnetite particles appear to have superior contrast (SNR as defined earlier ~23dB), the albumin microspheres also show promise as a contrast agent (SNR ~14dB). It is also interesting to note that the magnitude of the magnetic signal appears to vary between distinct regions throughout the tissue, suggesting either a difference in the ability of the agents to reach certain areas, or possibly a difference in the visco-elastic property of the tissue.

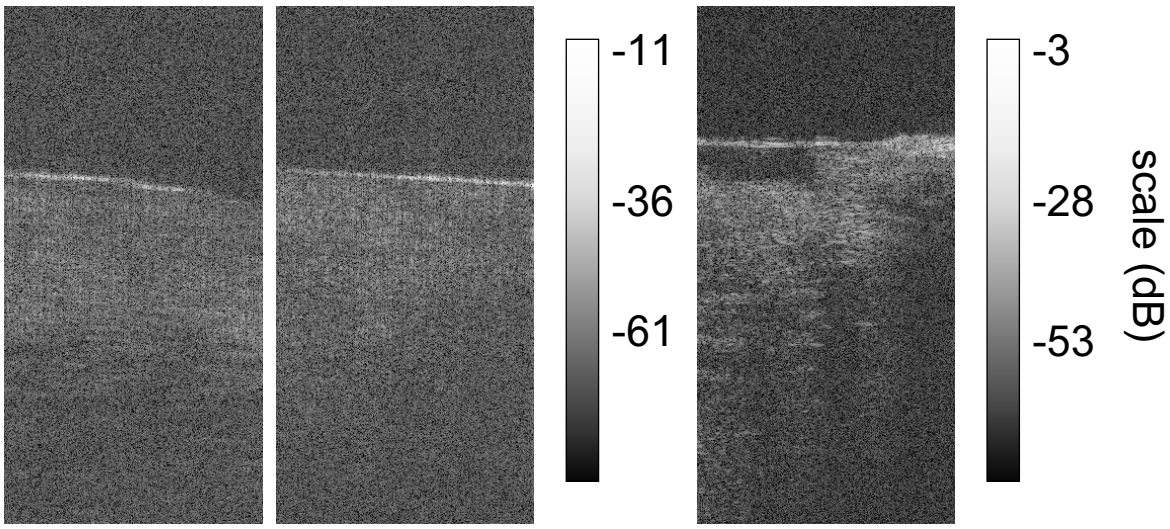

Fig. 6. Magneto-mechanical OCT images from chicken skin. Left: Control. Middle: Doped with albumin microspheres encapsulating magnetite colloid. Right: Doped with magnetite particles. The scale bar indicates the logarithmic scaling of the images, with zero referenced to 100% modulation of a pixel at the maximum intensity.

An *in vivo Xenopus laevis* tadpole model was employed to test the feasibility of these agents for *in vivo* magnetic detection. Early stage tadpoles were exposed to magnetite powder in their water for 24 hours prior to imaging. Since *Xenopus* tadpoles can filter sub-micron particles with their suction feeders it was expected that the magnetite-exposed tadpoles would contain significant amounts of magnetite powder in their digestive tract. Both magnetite-exposed and control tadpoles were anesthetized in a 0.5% benzocaine solution immediately prior to imaging. Tadpoles were imaged on both the ventral and dorsal side, throughout the body, and in all cases the control tadpoles showed no change in the magnetic-specific signal when the field was completely off versus modulated. However, as shown in Fig. 7, there was significant background signal in many of the control images, which is likely attributed to the constant motion inherent to living tissue. Since this technique is sensitive to motion on the 1μm scale, it may be difficult to avoid this effect without longer integrating times (to effectively bandpass filter) or the use of a faster scanning delay arm which would effectively freeze the biological motion.

We were able to verify the efficacy of magnetic imaging *in vivo* by comparing the magnetic-specific images obtained with the field completely off versus modulating with alternate A-lines. It appears that the tadpoles exposed to magnetite have significant magnetic signal improvement when the modulating field is applied, as shown in Fig. 7. The locations of greatest signal enhancement seem to correspond to the location of the gills (middle row) and stomach (bottom row); however this is a preliminary finding that warrants further investigation.

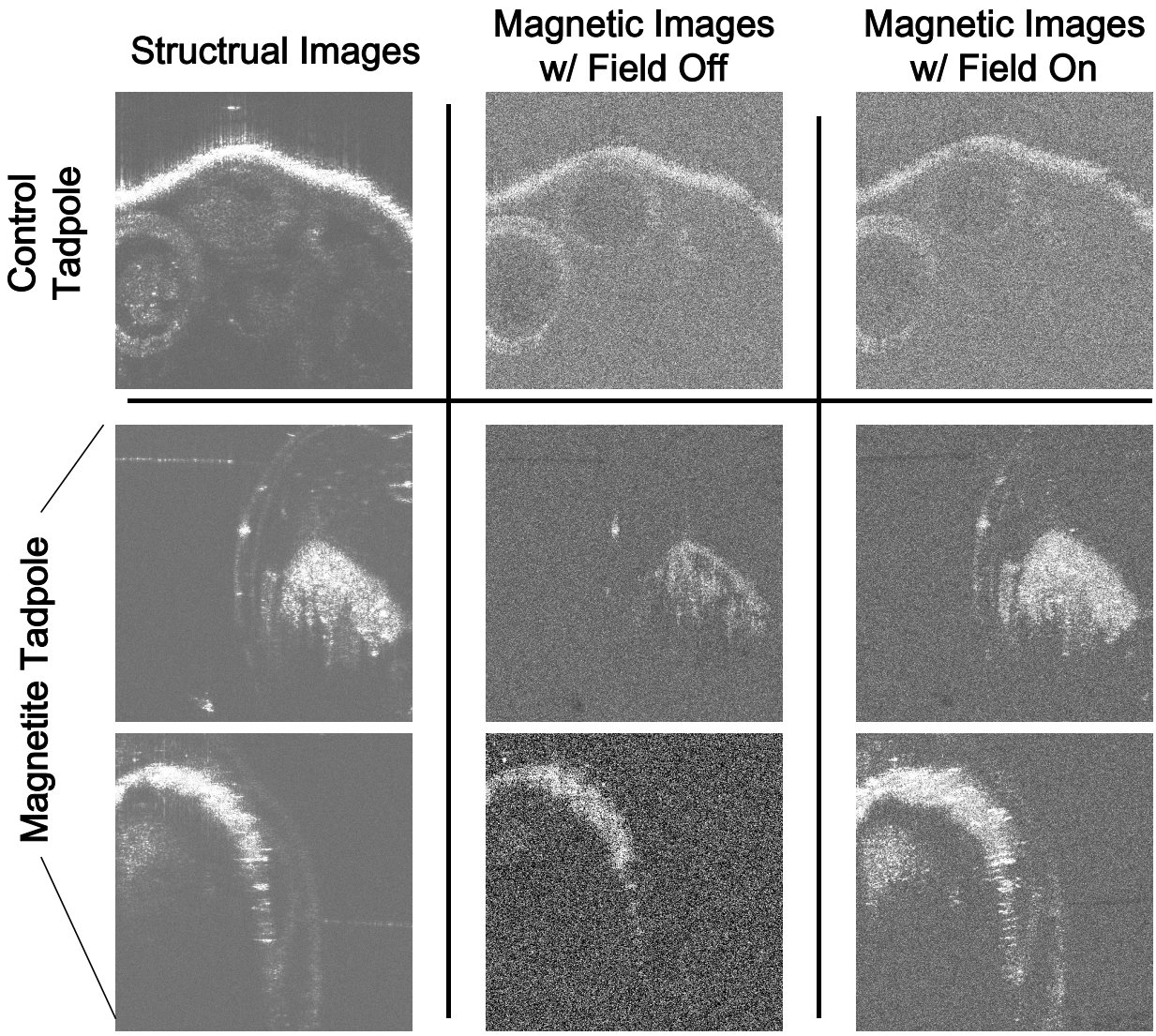

Fig. 7. OCT images (1mm x 1mm) of anesthetized *Xenopus laevis*. Left column: Structural OCT images. Middle column: Magnetically-processed OCT images obtained with the power to the solenoid off. Right column: Magnetic images with the magnetic field modulated. Top row: OCT Images of a control tadpole which was not exposed to magnetic contrast agents. Middle and bottom rows: OCT Images of a tadpole exposed to magnetite powder for 24 hours prior to imaging. A clear improvement of the magnetic images is obtained only in tadpoles exposed to magnetic contrast agents.

4. CONCLUSION

These results demonstrate that magnetic agents have promise as a novel class of contrast agent for OCT. By looking at changes in structural OCT images between the on and off states of an applied magnetic field, magnetic contrast agents can be localized with a signal-to-background ratio of ~23dB. We demonstrate that magnetic-specific imaging is feasible using *in vitro* cells and tissues as well as an *in vivo* tadpole. Although generally this technique is insensitive to

background structures, in practice it was found that the motion inherent to living tissue increased the background noise, requiring that one either scan at a faster rate to freeze this biological motion, or to integrate over a longer time in order to bandpass filter the motion from the magnetic-specific signal. Further investigations will focus on understanding the mechanism (translation vs. rotation) of the magnetomechanical motion and its dynamics as the switching frequency is increased. This technique may have future application in targeted imaging studies where background-free knowledge of the location of the contrast agents elucidates molecular information about the system.

ACKNOWLEDGEMENTS

This research was supported by The Whitaker Foundation (RG-01-0179), NIH (1 R01 EB00108-1), and jointly by NASA and the National Cancer Institute (NAS2-02057). We also thank Professor Andrew Webb and Wei Luo from the University of Illinois at Urbana-Champaign for their technical assistance.

REFERENCES

1. R. K. Wang and J. B. Elder, "Propylene glycol as a contrasting agent for optical coherence tomography to image gastrointestinal tissues", *Lasers Surg. Med*. **30**, 201-208, 2002.
2. J. R. Allport, R. Weissleder, "In vivo imaging of gene and cell therapies", *Exp. Hematol.* **29**, 1237-1246, 2002.
3. J. K. Barton, J. B. Hoying, C. J. Sullivan, "Use of microbubbles as an optical coherence tomography contrast agent", *Acad. Radiol.* **9S**, 52-55, 2002.
4. T. M. Lee, A. L. Oldenburg, S. Sitafalwalla, D. L. Marks, W. Luo, F. Jean-Jacques Toublan, K. S. Suslick, and S. A. Boppart, "Engineered microsphere contrast agents for optical coherence tomography", *Opt. Lett*. **28**, 1546-1548, 2003.
5. U. Hafeli, W. Schutt, J. Teller, M. Zborowski, eds., *Scientific and Clinical Applications of Magnetic Carriers*, Plenum Press, New York, 1997.
6. J. N. Anker and R. Kopelman, "Magnetically modulated optical nanoprobes," Appl. Phys. Lett. **82**(7), pp. 1102-1104, 2003.
7. S. Hamaguchi, I Tohnai, A. Ito, K. Mitsudo, T. Shigetomi, M. Ito, H. Honda, T. Kobayashi, M. Ueda, "Selective hyperthermia using magnetoliposomes to target cervical lymph node metastasis in a rabbit tongue tumor model", *Cancer Sci.* **94**, 834-839, 2003.
8. L. Levy, Y. Sahoo, K.-S. Kim, E. J. Bergey, P. N. Prasad, "Nanochemistry: Synthesis and characterization of multifunctional nanoclinics for biological applications", *Chem. Mater*. **14**, 3715-3721, 2002.
9. M. A. McDonald, K. L. Watkin, "Small particulate gadolinium oxide and gadolinium oxide albumin microspheres as multimodal contrast and therapeutic agents", *Invest. Radio*. 38, 305-310, 2003.
10. K. S. Suslick, "Sonochemistry and Sonoluminescence," In *Encyclopedia of Physical Science and Technology*, 3rd ed, Academic Press, **17**:363-376, 2001.
11. A. Ashkin, J. M. Dziedzic, J. E. Bjorkholm, Steven Chu, "Observation of single-beam gradient force optical grap for dielectric particles", *Opt. Lett*. **11**, 288-290, 1986.
12. P. A. Valberg and J. P. Bulter, "Magnetic particle motions within living cells", *Biophys. J*. **52**, 537-550, 1987.
13. D. L. Marks, A. L. Oldenburg, J. J. Reynolds, S. A. Boppart, "Study of an ultrahigh-umerical-aperture fiber continuum generation source for optical coherence tomography", *Opt. Lett.* **27**(22):2010-2012, 2002.